Petrographic study of coarse aggregate to evaluate their susceptibility to Alkali Silica Reactivity in different rocks of District Shangla, Swat, Pakistan

Asghar Ali[1], Muhammad Sajid[1], Liaqat Ali[2] and Mohammad Usman[3]
[1]Department of Geology, University of Peshawar, Pakistan
[2]National center of Excellence in Geology, University of Peshawar, Pakistan
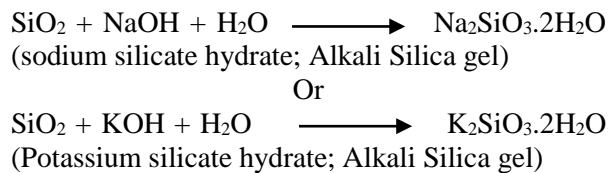[3]BAK Consulting Engineer, Peshawar, Pakistan

Abstract

Detailed petrographic investigation for identifying reactive silica in the form of microcrystalline, cryptocrystalline, amorphous, polycrystalline and undulose quartz in natural aggregate are extremely vital for prognosis of Alkali Silica Reactivity (ASR) before using them in high performance concrete. In active orogenic belt hydrothermal fluids alter feldspar and plagioclase into extremely fine grained quartz and mica in the form of muscovite or sericite by sericitization while the same fluids alter biotite and garnets into chlorite by chloritization. Similarly the intergrowth reaction between plagioclase and k-feldspar produces fine blebs of quartz by myrmekitization, which is extremely susceptible to ASR. Petrographic study indicates the occurrence of microcrystalline, polycrystalline, micro-fractured, strained and angular quartz grains plus the sillimanite protrusion in quartz make the aggregate samples extremely vulnerable to deleterious ASR. The protrusion of fibrolitic sillimanite from biotite into quartz is alarming because it creates tiny microscopic fractures, which can make the affected quartz grains extremely susceptible to ASR in the presence of alkali dissolved water. Additionally phyllosilicates including micas and chlorite are vulnerable to expansion by absorbing water that could potentially exert pressure on concrete bounded surfaces. Initial cracks on the surface of concrete due to expansion of these layered silicate minerals can provide channel paths for more water circulation in the concrete, which can further bulge muscovite, biotite, chlorite and alkali silica gel plus enhance the alteration of alteration sensitive minerals. Therefore, this study indicates that the rocks in the investigated areas predominantly consist of multiply deformed metamorphic and igneous rocks with high alkali silica reactivity (5-50%) and have exceeded International threshold limit. It is concluded from the current work that the coarse aggregate from metamorphic and igneous rocks of Shangla district, Swat are not recommended for high performance concrete and construction related activities.

Keywords: Aggregates; Petrography; Alkali Silica Reactivity.

1. Introduction

The total amount of cement in concrete can be reduced by using 50 to 80 percent aggregates (Kumar, 2006). Local availability of aggregates at construction sites potentially reduces transportation and labor costs. Using appropriate aggregates in concrete enhance the durability and strength of civil structures such as dams, bridges and highways (Aitcin, 2003; Fatt et al., 2013). However, aggregates susceptible to Alkali Silica Reactivity (ASR) may dramatically reduce durability, strength and performance of concrete that initiates in the concretes having reactive silica in the form of microcrystalline, cryptocrystalline, amorphous and undulose quartz in natural aggregate and adequate alkalis

(Na^+, K^+) in cement (Hobbs, 1990; Gilbert, 1995; Ponce and Batic, 2006). This reaction produces unstable alkali silica gel in the pore spaces of concrete when alkali hydroxides (NaOH and KOH) react with reactive silica. In the presence of moisture in air or imbibing water from other sources the alkali silica gel expands by swelling, which potentially leads to random cracking and expansion of concrete (Prezzi et al., 1997). Cracks in concrete further enhance water circulation within concrete causing alkali silica gel swelling and may initiate new ASR. Premature cracks in concrete dramatically reduce serviceability of high performance concrete structures. Alkali Silica Reaction takes place in the following ways in cement paste (Farny, 1996; Touma, 2000):

$SiO_2 + NaOH + H_2O \longrightarrow Na_2SiO_3.2H_2O$
(sodium silicate hydrate; Alkali Silica gel)

Or

$SiO_2 + KOH + H_2O \longrightarrow K_2SiO_3.2H_2O$
(Potassium silicate hydrate; Alkali Silica gel)

Aggregates prone to ASR can be well understood by petrographic technique. Petrographic investigations at microscopic scale of rock aggregates allow substantiating the presence and amount of reactive constituents that may cause deleterious damage (Berube and Fournier 1993; Gilbert, 1995). Therefore, petrographic analyses of aggregates are extremely vital for prognosis of ASR before using them in high performance concrete because acidic igneous, quartz rich metamorphic and sedimentary rocks have substantial amount of cryptocrystalline, microcrystalline, fractured, anhedral and highly strained quartz (Desai, 2010). Similarly the presence of biotite, muscovite/sericite and chlorite in these rocks make the aggregate susceptible to expansion by absorbing water. The minerals vulnerable to alteration for example feldspar, plagioclase, pyroxene and amphibole can potentially decrease the durability and strength of concrete. This study describes the use of petrographic analyses of 20 samples from Ghorband Khwar Shangla district, Swat to diagnose the vulnerability of aggregate samples to possible ASR before using them in concrete structures.

2. Geology of the study area

Northern Pakistan comprises of three tectonic domains from south to north, the Indian Plate, Kohistan Island Arc (KIA) and Eurasian Plate. The Kohistan Island Arc formed by the subduction of the Tethys during the Cretaceous. It collided with the Indian plate along the Main Mantle Thrust (MMT) during the Early to Mid Eocene (Fig. 1; Coward et al., 1986; Searle et al., 1999; DiPietro and Lawrence, 1991) and the Main Karakoram Thrust (MKT) during the Late Cretaceous (Searle et al., 1999; Shaltegger et al., 2002). The study area is located in the Beesham Complex ~10 km southeast of the MMT at the northern extreme northern margin of the Indian Plate. The Early Proterozoic Beesham Complex, which comprises of hornblende-biotite granodiorite gneiss, leucogranite, pegmatites, biotite orthogneiss and mafic intrusion is overlain by the Early to Late Proterozoic rocks collectively termed as Karora group (Treloar et al., 1989). The Karora

group consists of graphitic schist, fine grained metapsammites and calcite, dolomite and tremolite marble. These rocks are intruded by the Early Paleozoic porphyritic Swat and Mansehra granitic gneisses (Kazmi et al., 1984). The Precambrian and Early Paleozoic rocks of the Indian Plate are unconformably overlain by the Late Paleozoic to Late Mesozoic sequence of the Alpurai group metasediments (Lawrence et al., 1989; DiPietro et al., 1993). These metasediments are metamorphosed up to upper amphibolite facies metamorphic conditions. The Alpurai group in the study area is bounded in the northwest by the Indus mélange (Fig. 1). The Indus mélange, which marks the MMT in the region, contains greenstone, phyllite, marble, ultramafics, serpentinite and talc-carbonate schist (Hussain et al., 2004). The Kohistan Island Arc, which thrust over along the MMT on the Alpurai group metasediments, consists of Kohistan Batholith, Chilas Complex and Kamila Amphibolite Belt. The Kohistan Batholith consists of diorite, granodiorite, trondjemite, granite, leucogranite, gabbro and meta-volcanics. The Chilas Complex comprises of gabbronorite, anorthosite, pyroxenite and diorite. The Kamila Amphibolite Belt contains amphibolite, plagiogranite, hornblendite and diorite.
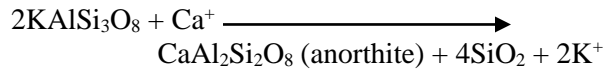
3. Methodology

20 representative samples including gneiss, schist, gabbro, granodiorite, granite, leucogranite, metapsammite and crystallized silica were selected for ASR from Ghorband Khwar in District Shangla. All the samples were examined in the field in hand specimen in order to collect representative samples for petrographic study from different locations in Ghorband Khwar. A total 20 thin sections were prepared form the representative samples and examined under Olympus polarizing microscope (Model NP – 400T) following the possible methodology of ASTM C295 for petrographic examination to identify alkali silica reactive constituents in them (ASTM, 1985).

4. Petrographic evaluation of aggregate samples for prognosis ASR
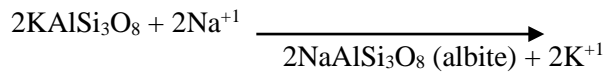
4.1. Myrmekitization

Intergrowth of extremely cryptocrystalline blebs/vermicules of quartz initiates at the common boundary of plagioclase and K-feldspar

phenocrysts due to myrmekitization (cf. Rong, 2002). During myrmekite formation aligned rod like microcrystalline quartz with rounded boundaries precipitates because of K-feldspar breakdown to more calcium rich plagioclase (anorthite) at high temperature (Becke, 1908; Collins, 1996; Rong, 2002). At higher temperature Ca in hydrothermal solution replaces K-feldspar in felsic rocks, which results into the production of calcium rich plagioclase and quartz.

$$2KAlSi_3O_8 + Ca^+ \longrightarrow CaAl_2Si_2O_8 \text{ (anorthite)} + 4SiO_2 + 2K^+$$

However, the replacement of K-feldspar by Na-plagioclase (sodic-plagioclase) does not liberate silica during myrmekitization.

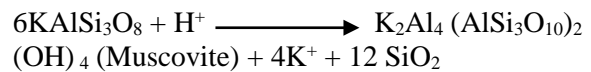$$2KAlSi_3O_8 + 2Na^{+1} \longrightarrow 2NaAlSi_3O_8 \text{ (albite)} + 2K^{+1}$$

During myrmekitization the release of potassium from K-feldspar initiates the formation of muscovite in the rock (Hatch et al., 1961). Myrmekite frequently occurred in felsic to intermediate igneous rocks, ortho/para granitic gneisses and quartzo-feldspathic schists. In these rocks the size of well-developed myrmekite ranging from 0.1mm to 0.5 mm, where the size of microcrystalline quartz vermicules varies in thickness from <0.005 mm to >0.015 mm (Rong, 2002).

4.2. Sericitization and chloritization

Hydrothermal alteration of alkali-feldspar and plagioclase commonly results into the formation of quartz and white mica in the form muscovite or paragonite, which are collectively, termed sericite due to sericitization (Que and Allen, 1996).

$$6KAlSi_3O_8 + H^+ \longrightarrow K_2Al_4 (AlSi_3O_{10})_2 (OH)_4 \text{ (Muscovite)} + 4K^+ + 12 SiO_2$$

This reaction extends from rims to the core in intensely deformed grains of feldspar and plagioclase. Circulation of hydrothermal solutions in addition to sericitization of plagioclase and feldspar also alters garnets, staurolite, pyroxene, amphibole and cordierite to chlorite by chloritization process.
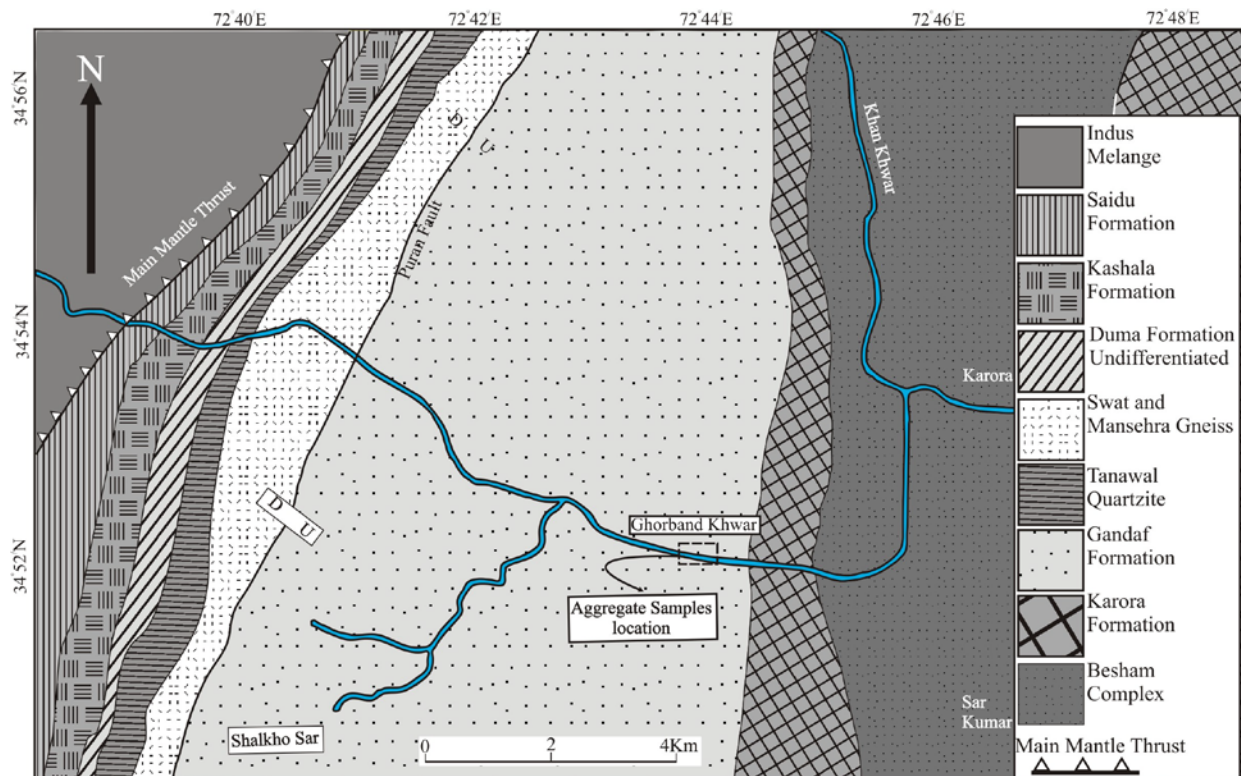

Fig. 1. Geological map of the area showing sample locations (modified Hussain et al., 2004 and BAK Consulting Engineers).

5. Petrographic examination of aggregate samples

Twenty samples were petrographically analyzed and their modal mineralogical composition and broader textural characteristics are presented in Table 1. The detailed petrographic characteristics of each of the rock types are described as:

5.1. Quartzo-feldspathic gneiss (04A)

The rock is formed by high-grade regional metamorphic differentiation processes from pre-exiting granite. Initially dispersed constituents of the granite are segregated into phyllosilicate rich (P-rich) and quartz-rich (Q-rich) domains. Muscovite and biotite segregated into the zones of non-coaxial deformation plus intense shearing (P/M-domain) while quartz and K-feldspar are concentrated into the zones of coaxial deformation (Q-domain). K-feldspar phenocrysts are characterized by inclusions of muscovite, biotite and quartz (Fig. 2a,c) and exhibit simple twinning. Recystallized elongate quartz grains arranged in the direction of phyllosilicate minerals (Fig. 2c,d). Strain shadows around K-feldspar phenocrysts occupied by microcrystalline silica, biotite and muscovite. Myrmekite that commonly occurs in the granite and granitic gneisses rimmed K-feldspar phenocrysts in the sample (Fig. 2b). K-feldspar phenocrysts are greatly replaced by myrmekites and mantled by recystallized quartz grains (Fig. 2c).
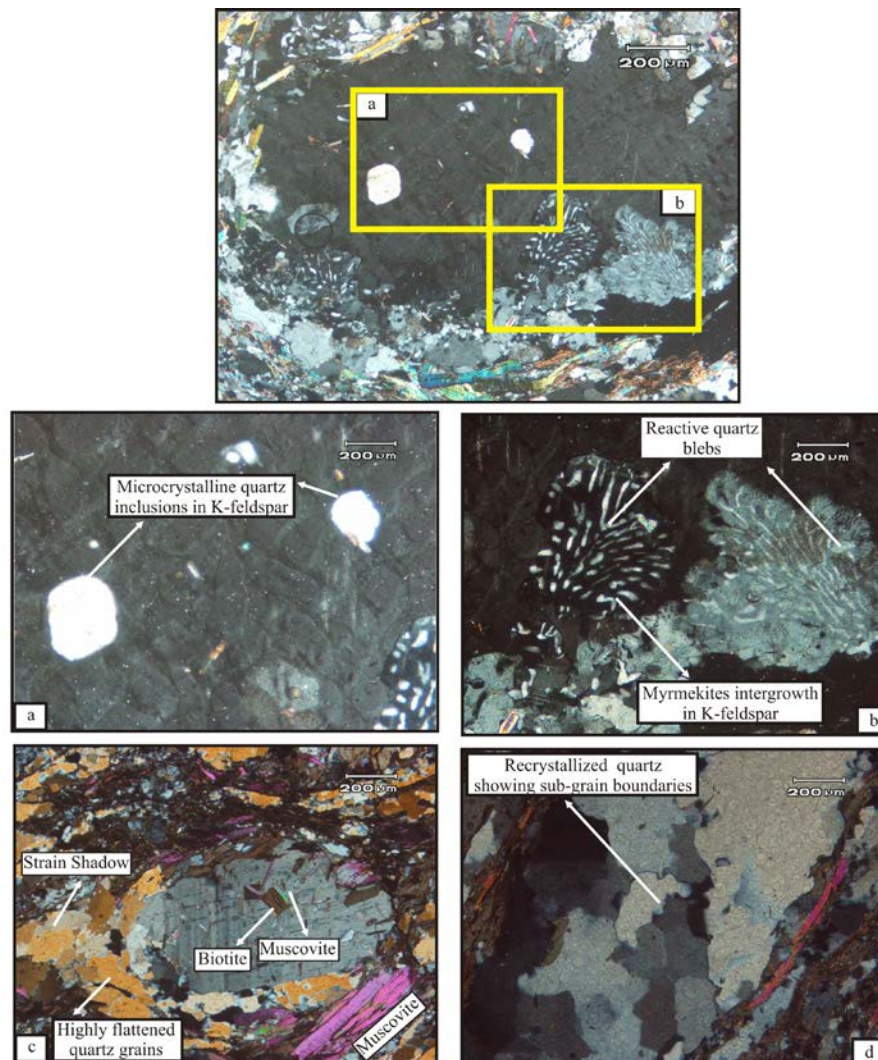

Fig. 2. Photomicrographs sample (04A). (a) Microcrystalline inclusions of quartz in K-feldspar phenocryst. (b) Myrmekite intergrowth of quartz blebs in K-feldspar. (c) Microcline feldspar contains inclusions of biotite and muscovite. Note the phenocryst is rimmed by fined grained muscovite and quartz. (d) Photomicrograph depicting anhedral recystallized quartz grain in the matrix. Most of the quartz grains in the rock are characterized by undulose extinction due to high strain.

128

Table 1. Modal Mineral composition of each sample, symbols of minerals are based on Kretz (1983). Quartz (Qtz), potash feldspar (Kfs), plagioclase (Pl), biotite (Bt), muscovite (Ms), garnet (Grt), kyanite (Ky), sillimanite (Sil), Pyroxene (Px), olivine (Ol), graphite (Gr), T (trace minerals).

S.#	Qtz	Kfs	Pl	Sericitized Kfs/Pl	Bt	Ms	Grt	Ky	Sil	Px	Ol	Gr	Opaque	Texture
04A	50			40	5	5							T	Gneissic
04B	25				5	45							25	Schistose
04C	35			35	20	10							T	Schistose
04D	70				20	T			10				T	Schistose
05A		38								60	2		T	Ophitic
05B	35			40	20	5	T		T					Gneissic
05C	80				15		3	T	T				2	Schistose
05D	50			35	5	5	T	T	T					Gneissic
06A	25	10	65											Granular
06B	10	70	15		3	2								Phaneritic
06C	35		3		35	5						20	2	Schistose
06D	55		25			20							T	Weak schistosity
07A	100													Massive
07B	55		10		15	20	T							Schistose
07C	65			5	20	5	5	T	T					Weakly foliated
07D	40		T		25	35	T						T	Schistose
08A	40	40	13			7							T	Phaneritic
08B	10				35	50							5	Schistose
08C	30	40	10		20	T	T			T				Gneissose
08D	30	40	10		20	T	T			T				Gneissose

S.#	Rock Name	Reactive constituents
04A	Quartzo-Felspathic Gneiss	Microcrystalline, amorphous, strained quartz, quartz blebs in myrmekites, quartz inclusions in phenocrysts
04B	Psuedomorphosed Muscovite Schist	Microcrystalline quartz in the matrix
04C	Quartzo-Feldspathic Mica Schist	Microcrystalline silica in the matrix, stained quartz, quartz blebs in myrmekites, quartz inclusions in sericitized phenocrysts
04D	Biotite Sillimanite Schist	Microcrystalline silica in the matrix, highly undulose/strained quartz
05A	Gabbro	Sericitization of plagioclase and alteration of pyroxene are possible
05B	Quartzo-Felspathic Gneiss	Microcrystalline, amorphous, strained quartz, quartz blebs in myrmekites, quartz inclusions in phenocrysts, sericitized fine grained quartz
05C	Sillimanite Kyanite Garnet Mica Schist	Microcrystalline quartz in the matrix, undulose elongated quartz
05D	Kyanite Sillimanite Quartzo-Feldspathic Gneiss	Microcrystalline, amorphous, strained quartz, quartz blebs in myrmekites, quartz inclusions in phenocrysts
06A	Granodiorite	Microcrystalline silica in the ground, anhedral strained quartz, plagioclase and k-feldspar are sericitized
06B	Granite	Microcrystalline, amorphous, strained quartz, quartz blebs in myrmekites, quartz inclusions in sericitized phenocrysts, microcrystalline rimmed phenocrysts
06C	Graphitic Quartz Mica Schist	Microcrystalline quartz in the matrix, highly stained quartz grains
06D	Metapsammite	Microcrystalline quartz in the matrix, stained undulose quartz, sericitized plagioclase
07A	Crystallized silica (SiO$_2$)	Phanerocrystalline quartz
07B	Garnet Mica Schist	Sericitized plagioclase, microcrystalline quartz matrix
07C	Kyanite Garnet Metapsammite	Microcrystalline quartz matrix, strained undulose quartz, sericitized plagioclase
07D	Garnet Mica	Microcrystalline
08A	Leucogranite	Quartz granoblasts, sericitized plagioclase and K-feldspar
08B	Quartz Mica Schist	Highly strained quartz grains, microcrystalline quartz in the matrix
08C	Quartzo-Felspathic Gneiss	Microcrystalline quartz inclusions in plagioclase, highly sericitized plagioclase and K-feldspar
08D	Quartzo-Felspathic Gneiss	Microcrystalline quartz inclusions in plagioclase, highly sericitized plagioclase and K-feldspar

5.2. Psuedomorphosed muscovite schist (04B)

The rock exhibits well developed schistosity. Strongly-oriented fine-grained quartz, opaque, biotite and muscovite define the dominant matrix foliations. Muscovite is much more abundant than biotite. Well developed muscovite psuedomorphs are numerous in the rocks and arranged in the direction of crenulation cleavages in the matrix. The identification of the psuedomorphosed mineral is difficult because that mineral has been completely replaced by fine grained muscovite (Fig. 3a). The psuedomorphs maintain the same shape across the thin section and are interpreted as being psuedomorphosed after a single mineral by muscovite. The psuedomorphs do not contain inclusions of opaque minerals, which indicate that the psuedomorphs predate the opaque minerals in the rock.

5.3. Quartzo-feldspathic mica schist (04C)

The differentiation between plagioclase and K-feldspar is difficult due to intense sericitization of these phases. However, the percentage of plagioclase and K-feldspar is much more than a normal pelitic rock. Therefore, the protolith is named after granite. Some K-feldspars are completely altered to dense fine cloudy mass. Least altered K-feldspar phenocrysts contain inclusions of muscovite, biotite and microcrystalline to cryptocrystalline quartz (Fig. 3b). Myrmekite at the boundary of K-feldspar resulted into fine grained quartz blebs and drops. Fine grained biotite and muscovite define the main schistosity. The matrix foliation deflects around phenocrysts of K-feldspar, plagioclase and quartz. Quartz grains are anhedral and intensely undulose.
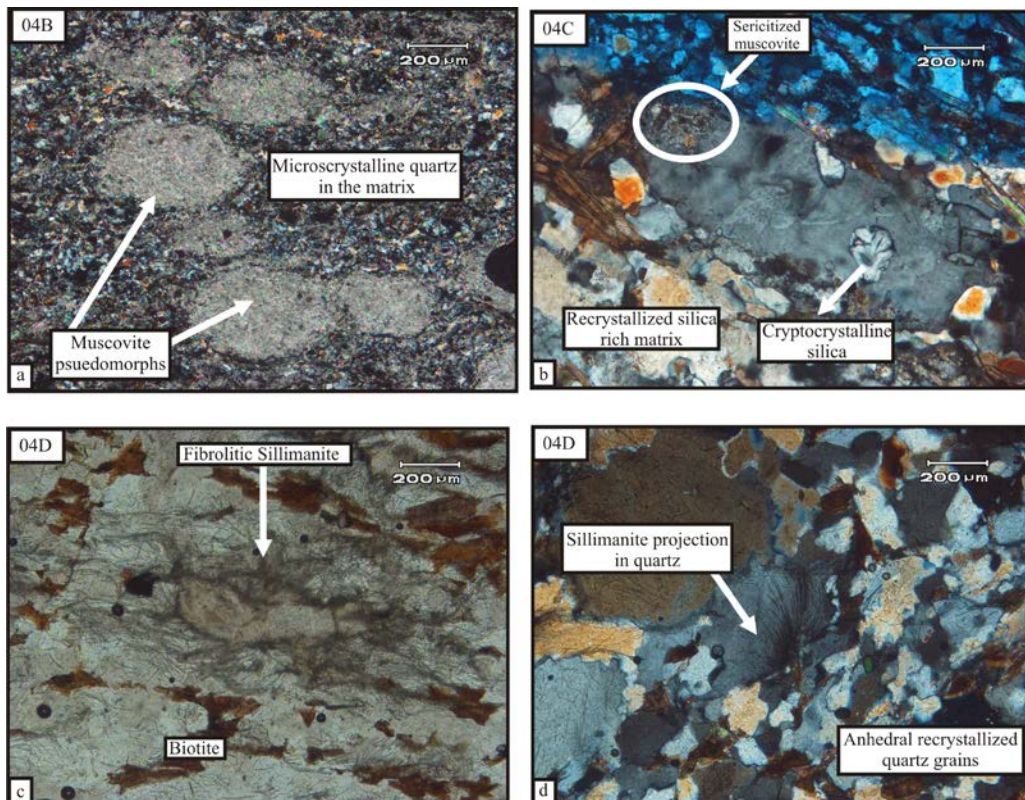

Fig. 3 a) Photomicrograph showing muscovite psuedomorphs after unknown mineral. The relics of the pre-existing mineral have been completely replaced by fine grained muscovite. b) Cryptocrystalline silica in K-feldspar and muscovite that formed by sericitization, c) Intergrown biotite and fibrolitic sillimanite and d) Sillimanite needles protrude into undulose quartz from the fine grained neighbor biotite.

5.4. Biotite sillimanite schist (04D)

Crenulation and crenulated cleavages in the rock are defined by biotite with alternating aligned quartz rich Q-domain. The presence of biotite is more than muscovite. The later phase is highly disseminated in the rock. Growth of fibrolitic sillimanite is embedded in biotite, quartz and fine grained muscovite (Fig. 3b, c). It is predominantly concentrated in the crenulation cleavages. The overprinting of biotite by fibrolitic sillimanite mostly resulted from the breakdown of biotite during regional metamorphism followed by higher grade of thermal metamorphism.

5.5. Gabbro (05A)

The rock exhibits well-developed ophitic texture where pyroxene encloses thin laths of plagioclase. Clinopyroxene and plagioclase phenocrysts are the dominant phases. Orthopyroxene do occur but is far lesser in amount than orthopyroxene, while olivine is present as a minor phase in the sample. The megacrystalline texture indicates that the rock crystallized from slow cooling of basaltic composition. The clinopyroxene is dominantly altered to chlorite as the result of chloritization. The rock is completely devoid of quartz, biotite, muscovite and K-feldspar.

5.6. Quartzo-feldspathic gneiss (05B)

The rock is formed by high-grade metamorphic differential processes from pre-existing coarse grained granite. Phenocrysts of biotite are poorly segregated into P-rich domain. K-feldspar contains inclusions of elongated muscovite, biotite and quartz. The contact between K-feldspars grains is occupied by cryptocrystalline silica, muscovite and myrmekite (Fig. 4c, d). K-feldspar Phenocrysts exhibit well-developed microcline cross-hatched twinning. Myrmekite is developed in the rim region of K-feldspar. Fibrolitic sillimanite grew in biotite and projects into quartz and k-feldspars. Fibrolitic Sillimanite has partially replaced biotite phenocrysts. Poikiloblastic garnet contains inclusions of quartz and fine grained biotite. Garnet in the sample has been formed from the chemical breakdown of biotite porphyroblast (Fig. 4a). Overall the matrix is dominated by anhedral and undulose quartz (Fig. 4b).

5.7. Sillimanite kyanite garnet mica schist (05C)

The regional metamorphic mineral assemblages indicate upper amphibolite facies metamorphism. Well-developed penetrative crenulation cleavages are concentrated by fine grained biotite. The rock consists of fine and coarse grained quartz grains, the recystallized course grained quartz grains are strongly aligned in the direction of crenulation cleavages (Fig. 5a). Garnet porphyroblasts, which contain inclusions of quartz and biotite, are arranged parallel to dominant crenulation cleavage. The inclusion trails preserved in garnet porphyroblasts are continuous with the main matrix crenulation cleavage. Fibrolitic sillimanite grew in biotite of crenulation cleavage and projects into garnet, kyanite and quartz. Later growth of kyanite porphyroblasts overprints the main crenulation cleavage. The main crenulation cleavage anastomoses against course grained recystallized undulose quartz grains, which indicate that the quartz grains predate the main matrix foliation.

5.8. Sillimanite kyanite quatzo-feldspathic gneiss (05D)

The rock is formed by the regional dynamothermal metamorphic conditions. The rock is dominated by highly reactive anhedral, microcrystalline and undulose quartz (Fig. 5b). K-feldspar has been broken-down into microcrystalline quartz and muscovite by sericitisation process. The sericitisation process is intense at K-feldspar and plagioclase lamellar twinning. Phenocrysts of K-feldspar exhibit well-developed microcline cross-hatched twinning while plagioclase phenocrysts are dominated by albite twinning. Biotite and muscovite are concentrated in the P-rich domain. Apart from main constituents, the rock also consists of garnet, kyanite (Fig. 5c) and fibrolitic sillimanite. Garnet porphyroblasts contain inclusions of biotite, muscovite and quartz. Fibrolitic sillimanite exclusively grew in biotite and projects in adjacent phases (quartz, feldspar etc).

5.9. Granodiorite (06A)

The rock sample exclusively consists of unaltered plagioclase. It displays well-developed albite twinning. Gneissic texture, biotite, hornblende, pyroxene, opaque and muscovite were not observed. Note these rocks are mainly

associated with active orogenic belts.

5.10. Granite (06B)

Equigranular crystals of K-feldspar are rimmed by muscovite and fine grained quartz. Some of K-feldspar and quartz are stretched up to 1cm in length perpendicular to tectonic shortening in ductile deformation. Phenocrysts of K-feldspar contain inclusions of elongated muscovite, biotite and quartz. Coarse grained quartz is highly undulose and anhedral. Coarse grained quartz is highly undulose and anhedral. The rock does not exhibit well-defined myrmekitic structure due to intense sericitization (Fig. 5 d, e). Muscovite and biotite are not segregated into cleavages. They are fine grained and highly disseminate. Chlorite replaces biotite due to hydrothermal alteration by chloritization process.
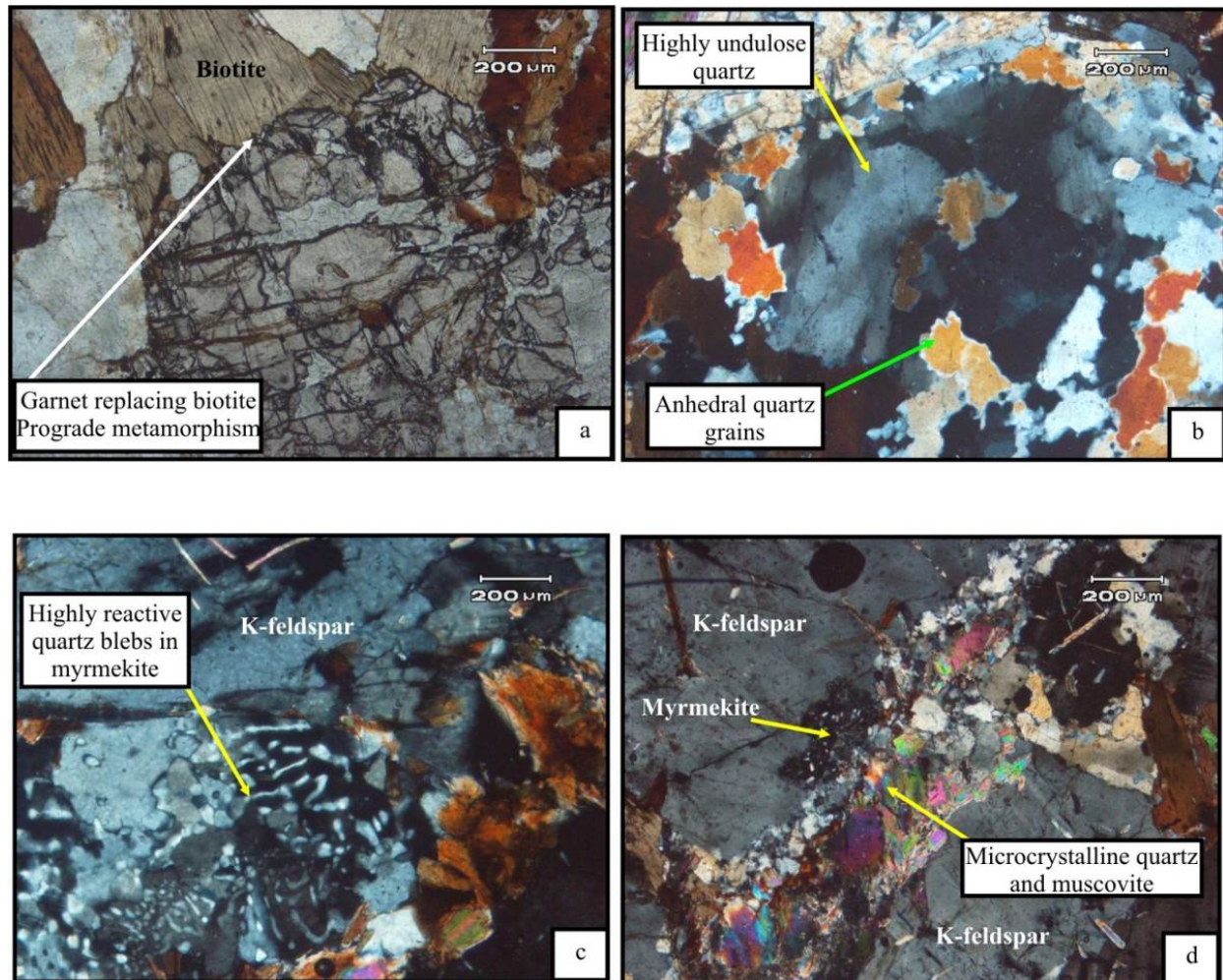

Fig. 4. Photomicrographs sample (05B). (a) Garnet porphyroblast containing inclusions of biotite and elongated quartz. Garnet is replacing biotite porphyroblast. (b) Highly undulose anhedral quartz in the ground mass. (c) Highly reactive quartz bleb in the myrmekite that grew at the rim of a K-feldspar. (d) Photomicrograph showing sericitized muscovite that produced from hydrothermal alteration of K-feldspar. Note the rim of K-feldspar in the left corner is characterized by myrmekite.
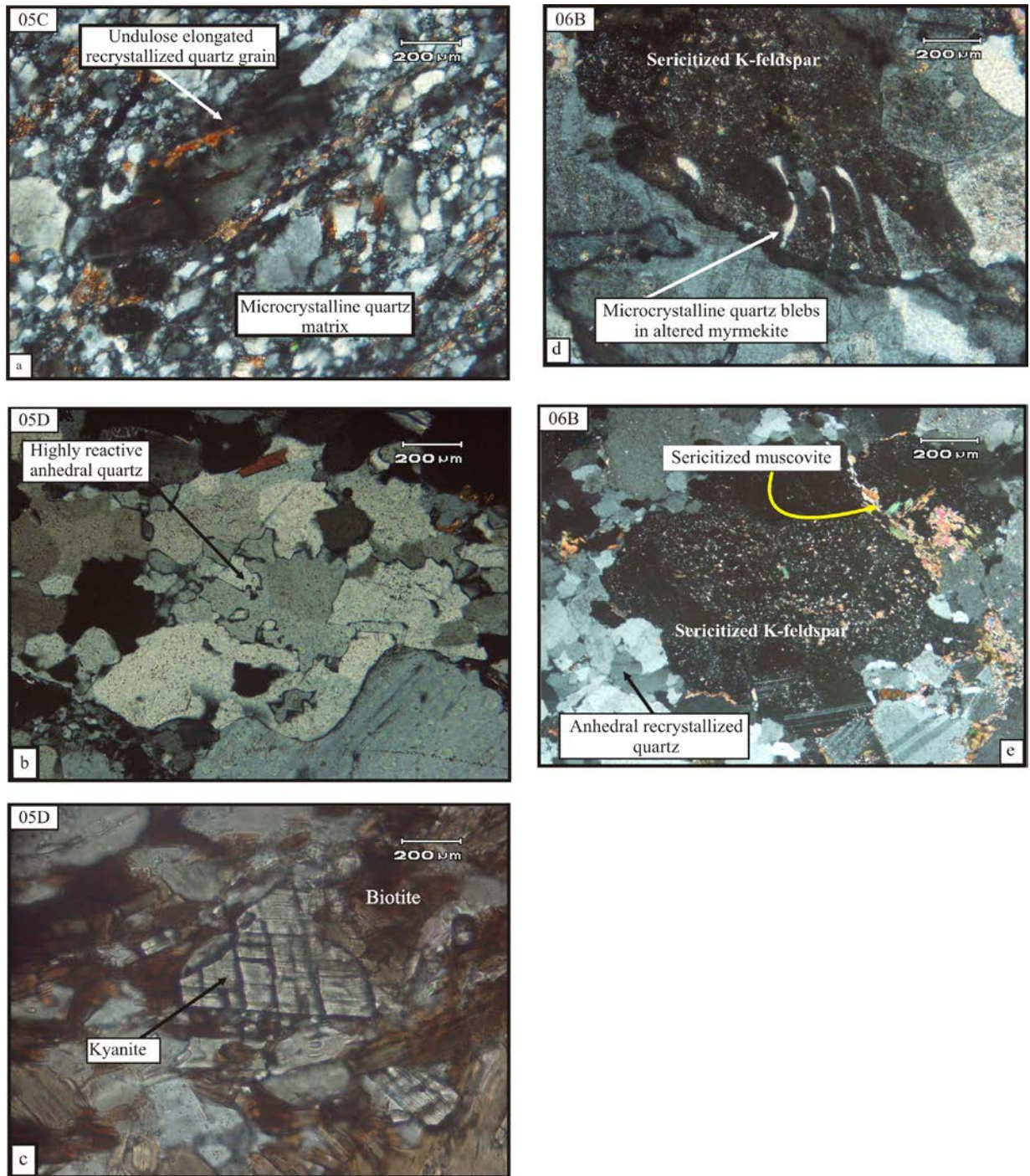
Fig. 5a) Photomicrograph showing undulatory extinction of elongated quartz grain aligned in the direction of crenulation cleavages. b) Highly reactive anhedral quartz grains. c) Photomicrograph illustrating kyanite porphyroblast in the rock. d) The plagioclase rich part of myrmekite is sericitized to fine grained muscovite while the more resistant quartz blebs are nicely visible. e) Photomicrograph of highly sericitized K-feldspar.

5.11. Graphite quartz mica schist (06C)

The Main schistosity is defined by graphite, fine grained muscovite and biotite (Fig. 6a). Graphite is highly concentrated in well-developed horizontal crenulation cleavages, which is later crenulated by young differential cleavage. Concentration of graphite increases towards the hinges of younger micro-folds. Due to intense deformation fine grained quartz and recystallized quartz grains are arranged in the direction of crenulation cleavages. Cleavages anastomosed around slightly sericitized plagioclase porphyroblasts. Plagioclase porphyroblasts contain inclusions of quartz. Fine grained biotite is wide spread in the sample while fine grained muscovite is mostly restricted to cleavage domains. Elongated and anhedral coarse grained quartz crystals exhibit undulose extinction (Fig. 6 b).

5.12. Metapsammite (06D)

The rock is fine grained and exclusively consists of quartz. A weakly developed crenulation cleavage is defined by fine grained muscovite. Plagioclase porphyroblasts are extremely sericitized due to hydrothermal fluids (Fig. 6c). Sericitization process resulted in growth of fine grained muscovite within plagioclase, which separated the sericitized phase from quartz grains in the matrix. Sericitization is much more abundant and severe at twin boundaries.

5.13. Crystallized silica (07A)

The crack has been simply filled with massive silica precipitated in the form of quartz from hot hydrothermal fluids. Phanerocrystalline quartz grains are fractured. The vein is void of ore minerals, muscovite, biotite and feldspar.

5.14. Garnet mica schist (07B)

Sub-idiomorphic plagioclase poikiloblasts contain inclusions of biotite, quartz and muscovite. They are rimmed by muscovite and fine grained quartz. The main matrix foliations anastomose around plagioclase poikiloblasts. Biotite and muscovite are present as well-aligned flakes in the main matrix foliation. The stain shadows around plagioclase are occupied by fined grained quartz. Garnet porphyroblasts contain inclusions of biotite, muscovite and quartz. Garnet

porphyroblasts poorly developed in the rock. Elongated quartz grains show undulose extinction.

5.15. Kyanite garnet metapsammite (07C)

Microscopic investigations show that the rock is mildly foliated. As a whole the rock is fine grained. Aligned phyllosilicates are too fine to see with the naked eye. Poikiloblastic garnets contain inclusions of muscovite, biotite and quartz. Quartz inclusions preserved in garnet porphyroblasts are coarser than those in the matrix. K-feldspar has locally been altered to quartz and fine grained muscovite. Biotite and muscovite are evenly distributed in the rock. Fibrolitic sillimanite grew only in biotite. Kyanite is extremely fine grained.

5.16. Garnet mica schist (07D)

Quartz is the most abundant phase in the rock. Elongate recystallized quartz and opaque minerals are aligned in the direction of the main matrix foliation. Elongated quartz grains exhibit undulose extinction. Garnet porphyroblasts contain inclusions of muscovite, biotite and quartz. Fine grained biotite and muscovite define the main crenulation cleavage. Foliations in the rock are visible at the mesoscopic scale. The matrix foliations are strongly intensified against garnet and coarse grained quartz rims. Only one grain of plagioclase was observed in the sample, which is highly sericitized.

5.17. Leucogranite (08A)

The rock is granitic in composition and light in colour. K-feldspar and plagioclase are highly sericitized. This process has produced fine grained muscovite around the rim of K-feldspar and plagioclase. Intense ubiquitous sericitization gives dull appearance to the rock. It is completely deficient in mafic minerals.

5.18. Quartz mica schist (08B)

The main matrix foliation defined by biotite and muscovite. It is kinked by younger deformation event (Fig. 6d). Due to intense deformation opaque minerals and stretched quartz are aligned parallel to muscovite and biotite. The matrix foliation intensifies against recystallized undulose quartz grains (Fig. 6e). Retrograde chlorite replaces biotite particularly in the cleavage domain.

5.19. Quartzo-feldspathic gneiss (08C)

Micro to mesoscopically the rock divided into alternating layers dark and felsic minerals. The dark mineral layers are dominated by biotite while the felsic layers substantially concentrated by K-feldspar, plagioclase and quartz. Sericitization process has produced extremely fine grained muscovite and quartz. Garnet porphyroblasts contains inclusions of quartz, muscovite and biotite. The rock displays well-developed gneissosity.

5.20. Quartzo-feldspathic gneiss (08D)

The rock displays well-developed gneissosity. Recystallized anhedral quartz grains are arranged in such a way that they provide granoblastic texture to the rock in the felsic layers. The dark mineral layers in the rock consist of biotite. K-feldspar and plagioclase phenocrysts are sericitized. Alternating felsic layers (bands) are ranging in width from 0.5cm up to 1cm. Phenocrysts are stretched in the direction of the main gneissosity.
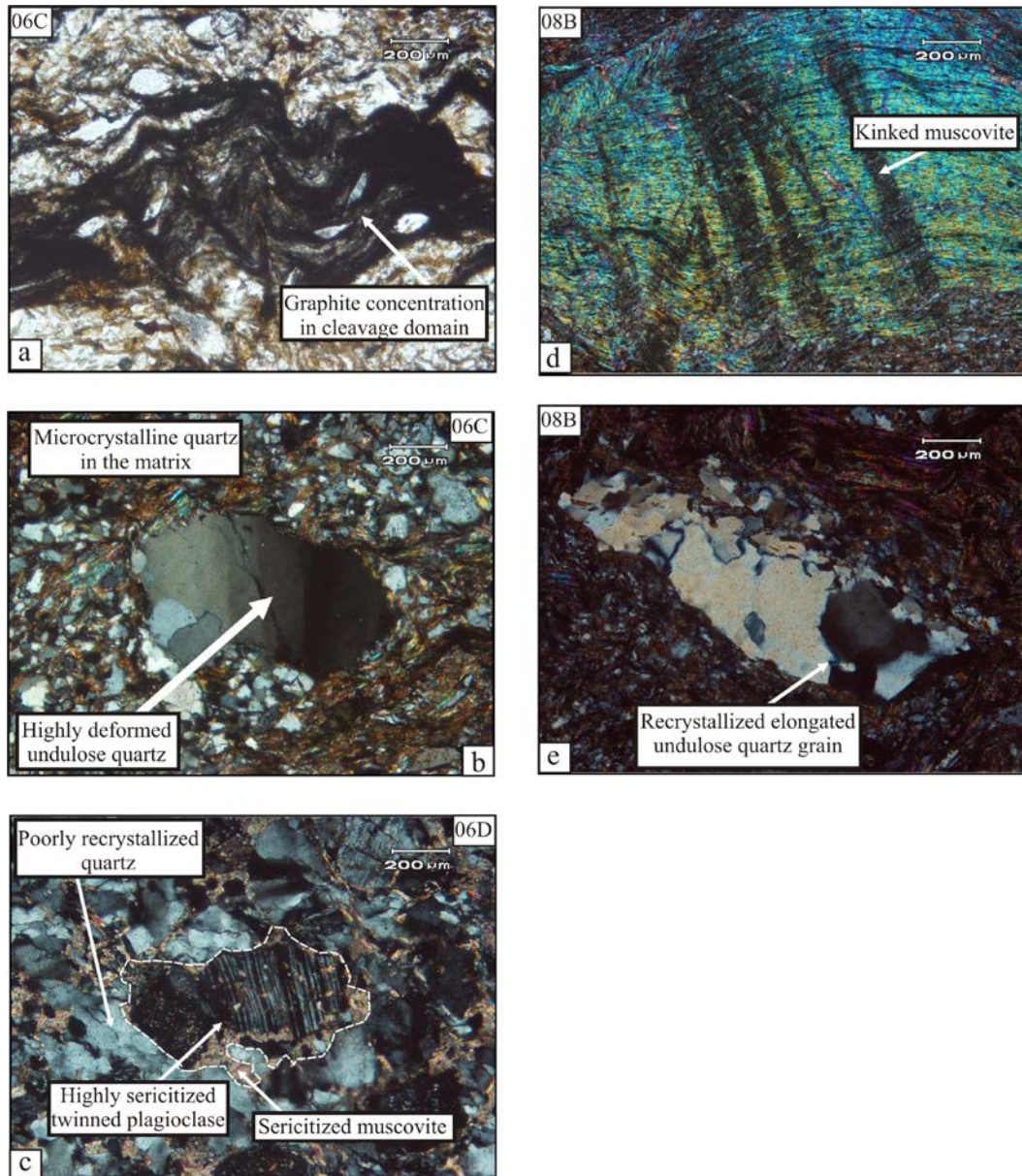

Fig. 6a) Photomicrograph illustrating the concentration of graphite in intensely deformed crenulation cleavage, b) Photomicrograph exhibiting fractured and undulose quartz grain embedded in the fine grained matrix, c) Photomicrograph showing highly sericitized grain of twinned plagioclase plus undulose extinction of an anhedral quartz grain, d) Photomicrograph showing micro-kinking in the muscovite dominated matrix foliation and e) Photomicrograph showing undulose extinction in deformed quartz grain.

6. Discussion

Detailed petrographic analyses provide incidence that the aggregate samples predominantly consist of quartz rich igneous and metamorphic rocks. Table 1 shows the petrographic summary and potentially reactive constituents of samples. Some reactions in these rocks have produced extremely reactive form of silica. For example the reaction between plagioclase and k-feldspar produced enormously fine blebs or drops of quartz. Similarly sericitization produced much fined grained muscovite and quartz. Muscovite and quartz occur on the boundary of K-feldspar and plagioclase phenocryst. High concentration of such reactive silica makes the provided aggregate samples vulnerable to ASR. Table 2 is highlighting National threshold limits of different countries where certain percentage of silica in aggregate could be considered reactive. According to the Mid-Atlantic Regional Technical Committee (Mid-Atlantic RTC, 1993) and AASHTO ASR Lead State Team (Lead State Team, 1999) aggregates for concrete should contain microcrystalline, strained undulose and microfractured quartz in the range of 0% to 5%. The chart shown in Figure 7 depicts percentage of reactive quartz in each sample.

Most of the samples predominantly consist of microcrystalline, polycrystalline, microfractured, strained, anhedral and elongated quartz grains. In addition, fine quartz blebs in myrmekites and amorphous (poorly crystalline) to microcrystalline quartz inclusions in highly sericitized plagioclase and K-feldspar may further enhance the ASR in the alkali rich cement paste. The high concentration of silica (SiO_2) makes these rocks extremely vulnerable to deleterious ASR after using with high performance cements. Such reactions can potentially lead to cracking and expansion of concrete. In reinforced concrete these cracks may potentially expose reinforced steel to expansion and corrosion, which might affect the serviceability of a structure. Microfractures in undulose and elongated quartz grains can potentially provide conduits for alkali solutions to migrate within cement paste to the most favorable reaction sites within the same grain.
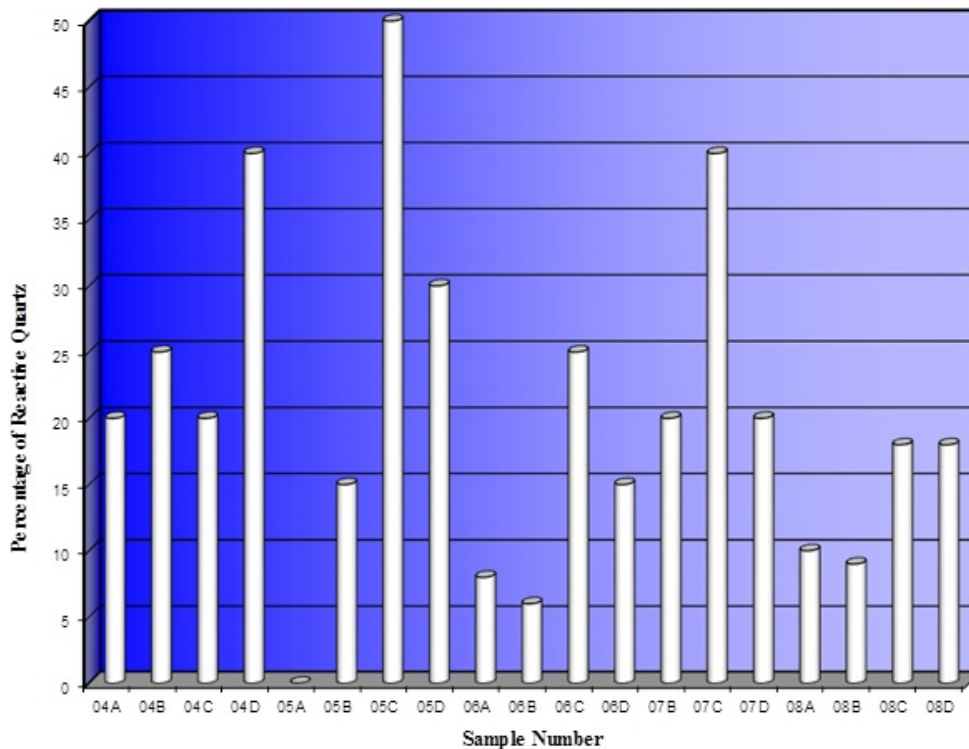

Fig. 7. Volume percentage of reactive quartz in 19 samples
Note: sample 7A is not mentioned on the chart because the aggregate was collected from quartz vein and lacking microcrystalline quartz grains.

136

Table 2. Threshold limit of silica reactivity in potentially reactive aggregates (after Rilem, 1993).

Country	Potentially reactive forms of silica in aggregate	Threshold of reactivity (% of Rock Material)
Belgium	Opal, Chalcedony, microcrystalline and cryptocrystalline quartz	<2%
Canada	Opal, tridymite, cristobalite, volcanic glasses, chalcedony, microcrystalline and cryptocrystalline quartz, macro-granular undulose quartz	As little as 1%
Denmark	Opal, cryptocrystalline quart	<2%
Ireland	I. Opal, cristobalite and tridymite II. Chalcedony, microcrystalline and cryptocrystalline quartz, volcanic glass	I. 0% II. <0.5%
Norway	Microcrystalline quartz	<2%
Russia	Opal, microcrystalline quartz, volcanic glass, cristobalite, tridymite, chalcedony	<5%
UK	I. Opal, cristobalite and tridymite II. Microcrystalline & cryptocrystalline quartz, strained quartz, Opal, Chalcedony, volcanic glass, III. Strained quartz	I. 0% II. <5% in fine aggregate III. <30%

Apart from high concentration of silica (SiO_2), these rocks also consist of abundant phyllosilicate minerals (biotite, muscovite and chlorite), which may easily swell up to the great extend by absorbing water or moisture. Swelling of phyllosilicate may exert enormous pressure at boundary between the cement paste and aggregate. This phenomenon can potentially generate cracks within the cement. Highly sericitized plagioclase and K-feldspar are potentially susceptible to alteration after using in high performance concrete. Some internally deformed garnet porphyroblasts contain inclusions of microcrystalline quartz, which may establish unstable reaction centers within the garnet porphyroblasts. The presence of kyanite and fibrolitic sillimanite in these samples indicates extreme metamorphic conditions across the regions. Sillimanite growth in quartz crystals makes the later phase susceptible to possible ASR.

7. Conclusions

In Pakistan very little research has been carried out on petrographic study in order to account for quality of coarse aggregate with respect to construction material. This study has highlighted the usefulness of petrographic study to evaluate the rocks of the Shangla district on the basis of alkali silica reactivity. Biotite sillimanite schist, sillimanite kyanite garnet mica schist and kyanite garnet metapsammite are showing high concentration of reactive silica exceeding the maximum threshold limit of strained quartz bearing aggregate (<30%) in the UK. Similarly other rocks in the area such as gneiss, schist, granodiorite, granite, leucogranite and cystallized silica being used for aggregate are also having high content of reactive silica (5 – 30%) exceeding the threshold limit of Belgium (<2%), Canada (~1 %), Ireland (<0.5%), Norway (<2 %), Russia (<5 %) and UK (<5%). Therefore, it is suggested that consideration should be given to detailed petrographic investigation for identifying alkali silica reactivity in coarse aggregates that are derived from the rocks exposed along the Indus Suture in other areas also with more or less similar lithologies.

References

Aitcin, P.C., 2003. The durability of high performance concrete: a review, cement and concrete composites. 25 (4-5): 409-420.

ASTM, 1985. Standard practice for petrographic examination of aggregates for concrete test designation C295-85. American Society for Testing and Materials.

Becke, F., 1908. Über Myrmekit: Mineralogie und Petrologie Mitteilung, 27, 377-390.

Berube, M.A., Fournier, B., 1993. Canadian Experience with Testing for Alkali Aggregate

Reactivity in Concrete. Cement and Concrete Composites, 15, 27-47.

Collins, L.G., 1996. Origin of myrmekite and metasomatic granite: Myrmekite, electronic Internet publication, no. 1, http://www.csun.edu/~vcgeo005/Nr1 Myrm. pdf.

Coward, M.P., Windley, B.F., Broughton, R.D., Luff, I.W., Petterson, M.G., Pudesy, C. J., Rex, D.C., Asif, K.M., 1986. Collision tectonics in the NW Himalaya. In: Coward, M.P., Ries, A. (Eds.), Collision tectonics, Geological Society of London Special Publication, 19, 203–219.

DiPietro, A.J., Lawrence D.A., 1991.Himalayan structure and metamorphism south of the Main Mantle Thrust, lower Swat, Pakistan. Journal of Metamorphic Geology, 9, 481-495.

DiPietro, A.J., Pogue, K.R., Lawrence, D.A., Baig, M.S., Hussain, A., Ahmed, I., 1993. Stratigraphy south of the Main Mantle Thrust, Lower Swat, Pakistan. Himalayan Tectonics, Special Publication, 74, 207–220.

Desai, P., 2010. Alkali Silica Reaction under the influence of chloride based deicers. Unpublished MS thesis, The Graduate School of Clemson University, 105.

Farny, J.A., 1996. Diagnosis and control of alkali-aggregate reactions in concrete. Portland Cement Association, American Concrete Pavement Association, Skokie, Illinois.

Fatt, N.T., Raj, J.K., Ghani, A.A., 2013. Potential Alkali-Reactivity of Granite Aggregates in the Bukit Lagongn Area, Selangor, Peninsular Malaysia. Sains Malaysiana, 42(6), 773–781.

Gilbert, S.T., 1995. Petrographic examination of samples of volcanic rocks from Anderson road quarries. Geo Special Project Report N. SPR 2/95.

Hatch, F.H., Well, A.K., Wells, M.K., 1961. Petrology of the igneous rocks. 12th edition Thomas Murby and Co, London, 1, 515.

Hobbs, D.W., 1990. Alkali-silica reaction. In *Standardsn for Aggregates,* edited by Pike, D.C. New York: Ellis Horwood.

Hussain, A., DiPietro, A.J., Pogue, R. K., Ahmad, I., 2004. Geological map of the 43B degree sheet, NWFP, Pakistan.

Kazmi, A.H., Lawrence, D.A., Dawood, H., Snee, L.W., Hussain, S.S., 1984. Geology of Indus suture in the Mingora-Shangla area of Swat, north Pakistan. Geological Bulletin, University of Peshawar, 17, 127–144.

Kretz, R., 1983. Symbols for rock-forming minerals. American Mineralogist, 68, 277–279.

Kumar S.P. 2006. A study on high performance concrete using sandstone aggregate. Unpublished Ph.D. thesis, School of Engineering and Information Technology, University Malaysia Sabah, 38.

Lawrence, R.D., Kazmi, A.H., Snee, L.W., 1989. Geological settings of emerald deposits of Swat, north Pakistan. In: Kazmi, A.H., Snee, L.W. (Eds.), Emeralds of Pakistan.

Ponce, M.J, Batic, R.O., 2006. Difference manifestations of the alkali-silica reaction in concrete according to the reaction kinetics of the reactive aggregate. Cement and Concrete Research, 36, 1148–1156.

Prezzi, M., Monteiro, P.J.M., Sposito, G., 1997. The Alkali Silica Reaction, Part I: Use of the double-layer theory to explain the behavior of reaction-product gels. ACI Material Journals, 94 (1), 10–18.

Que, M., Allen, R., 1996. Sericitization of plagioclase in the Rosses Granite Complex, Co. Donegal Ireland. Mineralogical Magazine, 60, 927–936.

Rilem, 1993. Code of practice for the petrographic analysis of the aggregates involved in the Alkali-Aggregate Reaction, Petrographic Working Group Report no RILEM/TC-106/93/08. RILEM (The International Union of Testing and Research Laboratories for Materials and Structures), 11.

Rong, J.S., 2002. Myrmekite formed by Na- and Ca-metasomatism of K-feldspar: Myrmekite, ISSN 1526-5757, electronic Internet publication, no. 45, http://www.csun.edu/~vcgeo005/Rn45Rong1.jpd.

Searle, M.P., Khan, M.A., Fraser, J.E., Gough, S. J., 1999. The tectonic evolution of the Kohistan-Karakoram collision belt along Karakom highway transect, north Pakistan. Tectonics, 18(6), 929–949.

Shaltegger, U., Zeilinger, G., Frank, M., Burg, J.P., 2002. Multiple mantle sources during island arc magmatism: U-Pb and Hf isotopic evidence from the Kohistan arc complex, Pakistan. Terra Nova, 14, 461–468.

Touma, E.W., 2000.Alkali Silica Reaction in portland cement concrete: testing methods and mitigation alternatives. Unpublished PhD thesis, The University of Texas At Austin, 556.

Treloar, P.J., Broughten, R.D., Coward, M.P., Williams, M.P., Windley, B. F., 1989. Deformation, metamorphism and imbrication of the Indian plate south of MMT, north Pakistan. Journal of Metamorphic Geology, 7, 111–127.